Published in final edited form as:
J Neurosci Methods. 2011 May 15; 198(1): 8–15. doi:10.1016/j.jneumeth.2011.02.021.

Simultaneous Detection of Cerebral Metabolism of Different Substrates by *in vivo* ^{13}C Isotopomer MRS

Yun Xiang and **Jun Shen***
Molecular Imaging Branch, National Institute of Mental Health Intramural Research Program, National Institutes of Health, Bethesda, MD, United States

Abstract

In this report a new method is introduced for simultaneous detection of the metabolism of two ^{13}C-labeled subtracts in brain *in vivo*. We recognized and experimentally demonstrated that when a ^{13}C-labeled substrate generates [1,2-$^{13}C_2$]acetylCoA ([1-^{13}C]acetylCoA) only, glutamate C5, glutamine C5 and apsartate C4 doublets (singlets) are formed exclusively, regardless of the number of turns of the tricarboxylic acid cycle. We utilized the large one-bond ^{13}C-^{13}C homonuclear *J* coupling between a carboxylic/amide carbon and an aliphatic carbon (~50 Hz) and demonstrated that it is feasible to simultaneously detect the labeling of brain metabolites by two different substrates using different isotopomer signals of the same carbon atom. Uniformly labeled glucose was used to generate the doublets and a second substrate ([2-^{13}C] lactate or [1,3-$^{13}C_2$]β-hydroxybutyrate or [1-^{13}C] acetate) was used to generate the singlets. It was shown that contribution to cerebral metabolism from different substrates can be simultaneously measured *in vivo*.

Keywords

cerebral energy metabolism; *in vivo* ^{13}C MRS; carboxylic/amide spectral region; ketone body; lactate

1. Introduction

Glucose is considered as the predominant energy substrate utilized by the mature brain to fuel its activities and functions (Pellerin and Magistretti, 2003). At rest, the adult brain comprising only about 2~3% of the body weight, accounts for approximately 25% and 16% of total body glucose and oxygen utilization respectively (Owen et al., 1967; Guzman and Blazquez, 2001; Henderson, 2008). Thus, glucose oxidation provides a major energy source for the brain function (Sibson et al, 1997; Pellerin and Magistretti, 2003). However, the brain does not use glucose as its only energy source (e.g., glycogen is found to be an energy reserve of significance; Cruz and Dienel, 2002; Choi et al, 1999), particularly during ontogenic development, fasting and diabetes. Under a variety of pathological conditions, ketone bodies including β-hydroxybutyrate (BHB) and acetoacetate (AcAc), lactate and free

*Corresponding author at: Jun Shen, PhD Molecular Imaging Branch National Institute of Mental Health Bldg. 10, Rm. 2D51A 9000 Rockville Pike, Bethesda, MD 20892-1527 Tel.: (301) 451-3408 Fax: (301) 480-2397 shenj@intra.nimh.nih.gov.

Disclosure/conflict of interest This work was supported by the Intramural Research Program of the National Institute of Mental Health, National Institutes of Health (NIMH-NIH). The authors have no conflict of interest to disclose, financial or otherwise.

fatty acids can be used as alternative fuels for energy production (O'Neal R et al., 1966; Lundquist et al., 1973; Hawkins, 1986; Edmond, 1992; Shen et al, 1998; Guzman and Blazquez, 2001; Lebon et al., 2002; Al-Mamun et al., 2009). Sometimes, even alcohol can act as an indirect or abnormal cerebral oxidative energy substrate in subjects of chronic alcoholism (Zakhari, 2006) due to its direct byproduct acetate being metabolized by glial cells in the brain. Even for glucose per se, there is still considerable controversy regarding compartmentalization of glucose oxidation (Aubert et al., 2005; Occhipinti et al., 2009; Cerdán et al., 2006). In recent decades, there has been a long-standing interest in compartmentalization, energy metabolism and neurotransmission in the brain. However, partly due to technical difficulties, the majority studies in this field have focused on detecting the cerebral metabolism of a single substrate in the brain (e.g., Cremer, 1964; O'Neal R et al., 1966; Hassel et al., 1995; Sibson et al, 1997; Waniewski and Martin, 1998), and few studies have investigated the simultaneous metabolism of multiple energy substrates.

The carbon-13 (^{13}C) nucleus, a stable isotope of carbon with 1.1% natural abundance, is nuclear magnetic resonance (NMR) detectable. ^{13}C magnetic resonance spectroscopy (MRS) combined with ^{13}C-labeled substrates allows for nonradioactive and noninvasive measurement of energy production and the metabolic fluxes in the brain because dynamic ^{13}C incorporation into the tricarboxylic acid (TCA) cycle and several different brain metabolites can be detected. Compared with in vitro or ex vivo ^{13}C NMR studies of brain extracts, *in vivo* ^{13}C MRS studies allow for continuous and nondestructive monitoring of ^{13}C incorporation from ^{13}C-labeled precursors into the various carbon positions of metabolites such as TCA cycle intermediates and amino acids under different physiological and pathophysiological conditions. The chemical shift of ^{13}C spans the alkyl (0~160 ppm) and carboxylic/amide (160~220 ppm) regions (Wilson, 1987; Rumpel, 2008), and the former especially the range from 20 to 60 ppm has been broadly used (Behar et al., 1986; Beckmann et al., 1991; de Graaf, 2007) for *in vivo* ^{13}C MRS. However, simultaneous detection of cerebral metabolism of two different substrates in the aliphatic ^{13}C spectral region is technically challenging because of the complex isotopomer signals generated by aliphatic carbons (e.g., Xu and Shen, 2006), which may lead to significant spectral overlap. In contrast to aliphatic carbons, carboxylic and amide carbons are located at an end of the carbon skeleton of a molecule. ^{13}C signals of carboxylic and amide carbons can only form a singlet (doublet) when its neighboring carbon is ^{12}C (^{13}C), leading to significant spectral simplification. Here we show that this natural spectral simplification can be utilized to simultaneously detect the metabolism of two ^{13}C-labeled subtracts in brain using *in vivo* ^{13}C MRS. We used uniformly labeled glucose to generate the doublets and a second substrate ([2-^{13}C] lactate or [1,3-$^{13}C_2$]BHB or [1-^{13}C] acetate) to generate the singlets and demonstrated that contribution to cerebral metabolism from different substrates can be determined *in vivo*.

2. Materials and Methods

2.1. Hardware

All MRS experiments were performed on a Bruker microimaging spectrometer (Bruker Biospin, Billerica, MA, USA) interfaced to an 11.7 Tesla 89-mm bore vertical magnet (Magnex Scientific, Abingdon, UK). This magnet is equipped with a 57-mm i.d. gradient (Mini 0.5; Bruker Biospin, Billerica, MA, USA) with a maximum gradient strength of 3.0 G/mm and a rise time of 100 μs for *in vivo* studies of adult rats. The ^{1}H and ^{13}C radio frequency (RF) coils were coplanar and made of single-sided printed circuit board. The inner loop is the ^{13}C coil, with an inner diameter and conductor width of 10.8 and 4.3 mm, respectively. The outer loop is the ^{1}H coil with an inner diameter and conductor width of 23.6 and 5.4 mm, respectively. No noise injection was found in the ^{13}C channel due to

proton decoupling. The lower end of the system was an aluminum interface box through which RF cables, ventilation tubes, rectal thermal probe, and catheters were connected. A similarly designed RF probe/animal handling system for proton and Proton-Observed, Carbon-13-Edited spectroscopy experiments of rat brain using this vertical magnet have been previously described (Li and Shen, 2005; Xu and Shen, 2006). The loaded isolation between ^{1}H and ^{13}C coils (S21), which have a large frequency separation of 375 MHz, is −30.6 dB at 125 MHz and −31.2 dB at 500 MHz, respectively, and the standard Bruker filters were used. A broadband low-pass filter was used in the ^{13}C channel whose insertion loss at 125 MHz was less than 0.5 dB. Its rejection at 500 MHz was greater than 80 dB. In the proton channel, a broadband high-pass filter was used with an insertion loss at 500 MHz of less than 0.5 dB, and rejection at 125 MHz greater than 60 dB. The integrated RF coils/head-holder system is capable of rat head fixation (with two ear pins and a bite bar), body support, physiology maintenance, coil tuning, and RF shielding. The pulse-acquire sequence (Li et al., 2009) was applied in the study to measure ^{13}C MRS signals in the rat brain with stochastic ^{1}H decoupling. Anatomical images were acquired using the three-slice (coronal, horizontal, and sagittal) scout rapid acquisition with Rapid Acquisition with Relaxation Enhancement (RARE) imaging method (field of view = 2.5 × 2.5 cm^2, slice thickness = 1 mm, TR/TE = 200/15 ms, rare factor = 8, data matrix = 128×128).

2.2. In vivo MR Procedures

After experimental animals were placed in the scanner, RARE images were acquired to ensure the animal brain and the RF coils were properly positioned. The gradient isocenter of the RF probe/animal handling system in a Mini 0.5 gradient was about 0–1 mm posterior to bregma. The rat brain was shimmed automatically using the FASTMAP/FLATNESS method (Chen et al., 2004) as described previously

A two-dimensionally localized stimulated-echo acquisition mode (STEAM) method was used to calibrate the proton pulse (Shen et al., 1999). Overhauser enhancement (NOE) between carboxylic/amide carbon and nearby protons (Pearson et al., 1975) was generated using a train of nominal 180° proton pulses spaced 200 ms apart. Because carbon in the carboxylic/amide carbon is only coupled to protons via very weak long-range ^{1}H-^{13}C scalar couplings, ^{13}C-labeled chemicals appearing in this chemical shift region can be effectively decoupled at a very low RF power using stochastic decoupling (Li et al., 2007; Yang et al., 2009). TR = 18.75s, Nominal flip angle = 45°. ^{1}H decoupling used a pseudo noise (stochastic) decoupling scheme with constant γB_2 amplitude and randomly inverted phases (Ernst, 1966; Li et al., 2007) and a repetition unit of 0.2–0.4 ms. The pseudo noise decoupling scheme allowed effective broadband proton decoupling at 11.7 T with a TR (18750 ms)-averaged forward decoupling power at < 6 mW (γB_2 < ~274 Hz calibrated at the gradient isocenter.). Our previous results have shown that this decoupling scheme can effectively decouple all protons that are coupled to the observed ^{13}C spins (from lactate H3 1.32 ppm to glutamine H_E at 7.60 ppm; Yang et al, 2009). All ^{13}C MRS data except for the baseline were acquired after the initiation of infusion of ^{13}C-labeled substrates. The time domain data were zero-filled to 16 K. The resolution enhancing exponential line broadening factor (lb = −15) and the Gaussian broadening factor (gb = 0.12) were applied before Fourier transform. Zero-order and a small first-order phase corrections were made.

2.3. Animal preparation

Animals were used in accordance to protocols approved by the National Institute of Mental Health (NIMH) Intramural Research Program Animal Care and Use Committee, National Institutes of Health (NIH). During the experimental process, all efforts were made to minimize animal suffering, to reduce the number of animals used, and to use alternatives *in vivo* techniques whenever available. Animals (adult Sprague-Dawley rats, Taconic

Laboratories, Germantown, NY, USA) were kept under conditions of constant temperature (21°C) and humidity (50%), with a 12-hour light/dark cycle and free access to food and water 24 hrs before the experiments. ^{13}C-enriched [$^{13}C_6$]-D-glucose and sodium [1-^{13}C]acetate were purchased from Cambridge Isotope Laboratories, Inc (Andover, MA, USA); sodium [1, 3-$^{13}C_2$]BHB and sodium [2-^{13}C]lactate solutions (45~55% w/w in H_2O) were obtained from Isotec., Sigma Aldrich (St. Louis, MO, USA). Enrichment of all ^{13}C-labeled chemicals was 99%.

All animals ((body weight (BW) = 193–237 g) fasted for 24 hrs were divided into seven groups from A to G. The rats were orally intubated and mechanically ventilated (SAR-830/AP, CWE, Inc., Ardmore, PA, USA) with a mixture of ~70% N_2O, 30% O_2 and 1.5% isoflurane. The left femoral artery was cannulated for periodically sampling arterial blood to monitor blood gases (pO_2, pCO_2), pH, and glucose concentration using a blood analyzer (Bayer Rapidlab 860, East Walpole, MA, USA), and for monitoring arterial blood pressure levels. The isolateral (left) vein was also cannulated for intravenous infusion or co-infusion of ^{13}C-labeled chemicals.

Three animals (Group A, n = 3) were given intravenous infusion of 0.75 M [$^{13}C_6$]-D-glucose. The intravenous infusion protocol consists of an initial bolus of 75.5 mg/min/kg BW of 0.75 M [$^{13}C_6$]-D-glucose in the first 10 min followed by the same solution at approximately 28.5 mg/min/kg BW. Plasma glucose level was constantly monitored and maintained at 16.0~19.0 mM. Animals in Group B (n = 3) received intravenous infusion of 0.6 M [2-^{13}C]lactate (pH = 7.0) with a initial bolus of 26.0 mg/min/kg BW followed by infusing the same solution at 10.2 mg/min/kg BW. Group C animals (n = 10) received intravenous co-infusion of 0.6 M [2-^{13}C]lactate and 0.75 M [$^{13}C_6$]-D-glucose. The glucose and lactate infusion protocols were the same as those for Group A and B respectively. Group D animals (n = 3) were used for intravenous infusion of 0.8 M [1, 3-$^{13}C_2$]BHB (pH = 7.0) with a initial bolus of 60.1 mg/min/kg BW followed by the same solution at 13.3 mg/min/kg BW. Animals in Group E (n = 9) received intravenous co-infusion of [$^{13}C_6$]-D-glucose and [1, 3-$^{13}C_2$]BHB. The glucose and BHB infusion protocols were the same as those for Group A and D respectively. Animals in Group F (n = 4) received intravenous infusion of 0.9 M [1-^{13}C]acetate (pH = 7.0) with a initial bolus of 18.7 mg/min/kg BW followed by infusion the same solution at 7.1 mg/min/kg BW. Animals in Group G (n = 10) were subjected to intravenous co-infusion of 0.9 M [1-^{13}C]acetate and 0.75 M [$^{13}C_6$]-D-glucose. The glucose and acetate infusion protocols were the same as those for Group A and F respectively. Throughout all experiments, normal physiological conditions were maintained according to results obtained from the blood analyzer (pH ~7.4, pCO_2 ~35 mmHg and pO_2 > 100 mmHg), respiration monitor (SurgicalVet, SIMS BCI, Inc. Wisconsin, USA), and by real-time regulation of ventilation. Alterations in blood pressure, heart rate, and respiration changes were also monitored (BIOPAC System, Inc. GenuineIntel, Goleta, CA). An external pump for heat exchange by circulating warm water (BayVoltex, Modesto, CA, USA) was used to maintain body temperature at 37.8 ± 0.5 °C.

3. Results

3.1. Intravenous infusion [$^{13}C_6$]-D-glucose and [2-^{13}C]lactate

Figure 1 shows *in vivo* proton decoupled ^{13}C MRS time-course spectra acquired from one Group A animal brain during intravenous infusion of [$^{13}C_6$]-D-glucose. Each spectrum corresponds to 20-minute signal averaging. ^{13}C MRS baseline from the rat brain (bottom trace) shows no detectable signals in the carboxylic/amide ^{13}C spectral region because there is no lipid interference in the spectral region of interest. Due to the homonuclear *J* coupling effect between the 4th and 5th ^{13}C from glutamate, glutamate C5 appears as a clear doublet in the carboxylic/amide ^{13}C spectral region. This is expected because the

glutamate ^{13}C4–^{13}C5 moiety always comes from [1,2-$^{13}C_2$]acetylCoA regardless of the number of turns of the TCA cycle. For example, in the second turn of the TCA cycle, glutamate C4–C5 is replaced by newly arrived ^{13}C-^{13}C from [1,2-$^{13}C_2$]acetylCoA. As a result, glutamate C5 singlet cannot be formed when [1,2-$^{13}C_2$]acetylCoA is the only labeled input to the TCA cycle. Glutamine C5 (178.5 ppm), and aspartate C4 (178.4 ppm) also appear as doublets because the covalent bond between the two carbons in [1,2-$^{13}C_2$]acetylCoA remains intact when these two ^{13}C labels are transferred to glutamine and aspartate. Glutamate C1 (175.3 ppm), aspartate C1 (175.1 ppm) and Glutamine C1 (174.8 ppm), however, can form both doublets and singlets although the two acetyl carbons of acetylCoA are derived from fully labeled [$^{13}C_6$]-D-glucose. This is because, when CO_2 is formed, the original covalent bond between the two acetyl carbons in acetylCoA is broken up. The break-off of CO_2 can lead to glutamate, glutamine and aspartate C1 singlets because the C2 carbons in these molecules may still be unlabeled. When glutamate, glutamine and aspartate are fully turned over, all carbons become ^{13}C-labeled. Therefore, glutamate, glutamine and aspartate C1 singlets are formed only during the $^{12}\text{C} \rightarrow {}^{13}\text{C}$ turnover period. With relatively long infusion time, all metabolites signals except bicarbonate are doublets in the carboxylic/amide spectral region. The ^{13}C-labeled bicarbonate HCO_3^- (161.0 ppm) was also detected (not shown in the figure). Similar results were obtained from all animals of group A. The glutamate C5, glutamine C5, aspartate C4 resonance peaks as well as the two largest peaks (Glu C1, Glu C1 +Gln C1 + Asp C1) in the C1 region were labeled in Fig. 1.

When [2-^{13}C]lactate entered into the brain, it is converted into [1-^{13}C]acetylCoA by the actions of lactate dehydrogenase and pyruvate dehydrogenase. The ^{13}C label is subsequently incorporated into glutamate C5 (182.0 ppm), glutamine C5 (178.5 ppm) and aspartate C4 (178.3 ppm) during the first turn of the TCA cycle. For exactly the same reason stated above, the glutamate ^{12}C4–^{13}C5 moiety always comes from [1-^{13}C]acetylCoA regardless of the number of turns of the TCA cycle. Therefore, glutamate C5, glutamine C5 and aspartate C4 doublets cannot be formed when [1-^{13}C]acetylCoA is the only labeled input to the TCA cycle. When [1-^{13}C]acetylCoA is the only labeled input to the TCA cycle glutamate, glutamine and aspartate C1 doublets cannot be formed, either. Fig. 2(a) shows *in vivo* proton decoupled ^{13}C MRS time-course spectra acquired from one Group B animal brain during intravenous infusion of [2-^{13}C]lactate. Only singlets were observed as expected. Fig. 2(b) shows the corresponding result of co-infusion of [$^{13}C_6$]-D-glucose and [2-^{13}C]lactate acquired from a Group C animal. In the co-infusion experiment, glutamate C5, glutamine C5 and aspartate C4 doublets are originated from [$^{13}C_6$]-D-glucose while glutamate C5, glutamine C5 and aspartate C4 singlets are originated from [2-^{13}C]lactate. Fig. 2(b) clearly demonstrated the feasibility of simultaneously detecting the metabolism of two different substrates if one substrate (e.g., [$^{13}C_6$]-D-glucose) only produces [1,2-$^{13}C_2$]acetylCoA and the other (e.g., [2-^{13}C]lactate) only produces [1-^{13}C]acetylCoA.

Fig. 3 shows ^{13}C MRS baseline and spectra accumulated over the 0–180 minutes infusion period. As expected, only singlets of glutamate, glutamine and aspartate were detected during intravenous infusion of [2-^{13}C]lactate; during intravenous infusion of [$^{13}C_6$]-D-glucose only doublets were detected for glutamate C5, glutamine C5 and aspartate C4. The same conclusion holds when spectra from all animals in Group A and B were summed respectively. The summed co-infusion spectrum demonstrates that co-infusion of differently labeled substrates and the detection of signals in the carboxylic/amide ^{13}C spectral region allow clear separation of contribution to glutamate, glutamine and aspartate from the different substrates. As shown by Fig. 2(b) and the co-infusion spectrum of Fig. 3, the large homonuclear ^{13}C-^{13}C *J* coupling between an aliphatic carbon and a carboxylic or an amide carbon and the lack of interference from other one-bond couplings allow a clear separation of signals originated from singly and doubly labeled substrates. At 11.7 Tesla, the chemical shift separation between glutamine C5 and aspartate C4 is one half of the one-bond *J*

coupling between an aliphatic carbon and a carboxylic/amide carbon. In Fig. 2(b) and Fig. 3, a pseudo quartet was detected in the 178–179 ppm region, allowing easy separation of contributions to glutamine C5 and aspartate C4 from different substrates. In the C1 region, singlets originated from singly labeled [2-^{13}C]lactate and doublets and singlets originated from [$^{13}C_6$]-D-glucose were detected in the summed co-infusion spectrum of Fig. 3.

3.2. Intravenous infusion of [$^{13}C_6$]-D-glucose and [1,3-$^{13}C_2$]BHB

Like [2-^{13}C]lactate, the ketone body [1,3-$^{13}C_2$]BHB is also converted into [1-^{13}C]acetylCoA in brain. Fig. 4 shows the *in vivo* ^{13}C MRS time-course spectra acquired from individual animals in Groups D and E, respectively. In Fig. 4(a), only singlets were generated in the carboxylic/amide ^{13}C spectral region. With co-infusion of [$^{13}C_6$]-D-glucose and [1,3-$^{13}C_2$]BHB glutamate C5, glutamine C5 and aspartate C4 doublets are originated from [$^{13}C_6$]-D-glucose; glutamate C5, glutamine C5 and aspartate C4 singlets are originated from [1,3-$^{13}C_2$]BHB (see Fig. 4(b)). Similar to co-infusion of [$^{13}C_6$]-D-glucose and [2-^{13}C]lactate, a pseudo quartet was detected in the 178–179 ppm region at 11.7 Tesla during co-infusion of [$^{13}C_6$]-D-glucose and [1,3-$^{13}C_2$]BHB. Similar results were also obtained for Group F and Group G animals.

3.3 Comparison of intravenous co-infusions of [$^{13}C_6$]-D-glucose, [2-^{13}C]lactate, [1,3-$^{13}C_2$]BHB and [1-^{13}C]acetate

Fig. 5 shows ^{13}C MRS spectra accumulated over the 0–180 minutes infusion period for three different co-infusion experiments: [$^{13}C_6$]-D-glucose + [2-^{13}C]lactate (top trace), [$^{13}C_6$]-D-glucose + [1,3-$^{13}C_2$]BHB (middle trace), [$^{13}C_6$]-D-glucose + [1-^{13}C]acetate (bottom trace). Among [$^{13}C_6$]-D-glucose, [2-^{13}C]lactate, [1,3-$^{13}C_2$]BHB and [1-^{13}C]acetate, [1-^{13}C]acetate is the only glia-specific substrates. [1-^{13}C]acetate labels glutamine C5 in glial cells first before the labels is transferred to neuronal glutamate. As a result in the bottom trace of Fig. 5, the signal intensity of glutamine C5 singlet is much higher than that of glutamate C5 singlet. In contrast, none of the rest of the substrates shows such a reversal of the precursor-product relationship between glutamate and glutamine. Quantitative analysis of the glutamate C5, glutamine C5 and aspartate C4 singlets and doublets revealed the expected brain's preference for glucose as the respiration fuel. At 180 min after the initiation of co-infusion, $[GluC5]_{Glucose}/[GluC5]_{Lactate}$, $[GlnC5]_{Glucose}/[GlnC5]_{Lactate}$ and $[GluC5 + GlnC5 + AspC4]_{Glucose}/[GluC5 + GlnC5 + AspC4]_{Lactate}$ ratios from Group C animals were found to be (4.23 ± 0.30, 7.50 ± 0.31, 5.11 ± 0.58):1 (see Table 1). The results for Group E and Group G animals were also listed in Table 1.

4. Discussion

4.1. Observation of cerebral metabolism by in vivo ^{13}C MRS in the carboxylic/amide region

In vivo ^{13}C MRS combined with the administration of ^{13}C-labeled substrates has become a powerful tool for studies of cerebral energy metabolism due to its nonradioactive and nondestructive features. In the present study, we tried to observe the cerebral metabolism of different energy substrates in the carboxylic/amide ^{13}C spectral region. The results showed that the major difficulties associated with decoupling the large ^{1}H-^{13}C scalar coupling (120–150 Hz) for alkyl carbons of multiple brain metabolites can be ignored in the carboxylic/amide ^{13}C spectral region because the carboxylic/amide carbons are only remotely coupled to protons. As such, complete decoupling was achieved using very low RF power. An additional advantage of this method is there are no overlapping signals from scalp lipids in the spectral region of interest (174–183 ppm) even when conventional localization techniques are not used. This is in contrast to the commonly used aliphatic ^{13}C spectral region where signals from scalp lipids dominate and may interfere with metabolite signals. Since carboxylic and amide carbons are located at an end of the carbon skeleton of a

molecule ^{13}C signals of carboxylic and amide carbons can only form a singlet or a doublet. This is in contrast to aliphatic carbons that may form complex ^{13}C isotopomer signals, leading to significant spectral overlap (Xu and Shen, 2006). The results of this study showed that the natural spectral simplification in the carboxylic/amide ^{13}C spectral region can be taken advantage of to simultaneously detect the metabolism of two ^{13}C-labeled subtracts in brain *in vivo*. The simultaneous detection of cerebral metabolism in the carboxylic/amide ^{13}C spectral region is further helped by the fact that the one-bond ^{13}C-^{13}C homonuclear *J* coupling between a carboxylic/amide carbon and an aliphatic carbon (~50 Hz) is quite larger than the homonuclear *J* coupling between two aliphatic carbons (~30 Hz). In our study we only used uniformly labeled glucose to generate glutamate C5, glutamine C5 and aspartate C4 doublets and another substrate ([2-^{13}C] lactate or [1,3-$^{13}C_2$]BHB or [1-^{13}C] acetate) to generate singlets. Other choices or combinations of substrates are also possible. As long as one substrate only generates [1,2-$^{13}C_2$]acetylCoA and the other only generates ([1-^{13}C]acetylCoA) simultaneous detection of cerebral metabolism of these two substrates in the carboxylic/amide ^{13}C spectral region can be performed using *in vivo* ^{13}C MRS.

In this study, signal intensity ratios (Table 1) were used to quantify brain's preference of respiration fuels (Malloy et al, 1988). For metabolic modeling of the kinetics of ^{13}C labeling of different istopomers absolulte quantification of the detected carboxylic/amide ^{13}C signals will be needed, which is beyond the scope of this report.

4.2. [2-^{13}C] lactate and [$^{13}C_6$]-D-glucose

Brain may not use glucose as the only energy source especially under pathological conditions such as hypoxia and ischemia. Lactate can become a significant fuel source and occupy a special position in energy metabolism of the brain, and it may be required energetically to support synaptic function (Prichard, 1991; Boumezbeur et al., 2010). The exact role of lactate in brain energy metabolism and glutamatergic neurotransmission has been controversial (Waagepetersen et al., 1998; Bouzier-Sore et al., 2006; Schurr, 2006; Uehara et al., 2008). Measuring lactate in the brain is important for studying blood flow, consumption of glucose and oxygen, and brain activities (Urrila et al., 2004; Mangia et al., 2009). MRS detection of lactate usually involves measuring its methyl proton signal at 1.32 ppm in proton MRS spectra. With intravenous infusion of [1-^{13}C] or [1,6-$^{13}C_2$]glucose the methyl carbon of lactate (C3, 21.0 ppm) can also be detected using conventional ^{13}C MRS that measures ^{13}C labels in the aliphatic ^{13}C spectral region (Shen et al., 1999). In our study, [2-^{13}C]lactate was administered. The lactate C2 signal at 69.3 ppm was also observed (data not shown). We found that cerebral metabolism of [2-^{13}C]lactate leads to ^{13}C labeling of glutamate, glutamine, aspartate and bicarbonate. Using [$^{13}C_6$]-D-glucose to generate [1,2-$^{13}C_2$]acetylCoA and [2-^{13}C]lactate to generate [1-^{13}C]acetylCoA our results showed that the metabolism of glucose and lactate in brain can be simultaneously measured. Table 1 showed that brains' selection of respiration fuels may be quantitatively measured by our *in vivo* ^{13}C MRS method. Comparing the accumulated ^{13}C MRS spectra with infusion of [2-^{13}C] lactate, [$^{13}C_6$]-D-glucose, and co-infusion of [2-^{13}C] lactate and [$^{13}C_6$]-D-glucose (Fig. 3 and Table 1), it is interesting to see that lactate has a significant contribution to brain energy metabolism even at the high blood glucose level of 18.5 ± 1.7 mM (Group C).

4.3. [1,3-$^{13}C_2$]BHB and [$^{13}C_6$]-D-glucose

A substantial body of evidence indicates that during ontogenic development, fasting and diabetes, ketone body including BHB, AcAc and acetone can serve as an alternative fuels for energy production in the brain (Shen et al, 1998; Magistretti et al., 1999; Guzman and Blazquez, 2001; Pan et al, 2002; Bouzier-Sore et al., 2003). Previous experimental and clinical studies confirmed that ketone bodies can be used to treat diseases such as epilepsy,

Alzheimer's disease, Parkinson's disease, Friedreich's ataxia, cerebral ischemia, and hypoxia (Guzman and Blazquez, 2001; Veech et al., 2001; Guzman and Blazquez, 2004). BHB is able to replace glucose as an energy substrate and to preserve neuronal integrity and stability during glucose deprivation or glycolytic inhibition (Nehlig, 2004). Because both BHB C1 and C3 become acetyl C1 carbon of acetylCoA we used [1,3-$^{13}C_2$]BHB to double the sensitivity of detecting BHB metabolism. The resonances of BHB C1 and C3 are located at 181.2 and 66.8 ppm. Its C1 peak can be appreciated in Figs. 4 and 5, which does not overlap with metabolite signals of interest. BHB is known to easily enter both neuronal and glial compartments. Previous tissue culture studies have estimated that (Sykes et al., 1986) approximately 60% of BHB entered into neurons is oxidized, whereas this is only 20% in glial cells. During the infusion of [1,3-$^{13}C_2$]BHB both glutamate and glutamine were found to be readily labeled by ^{13}C (Fig. 4(a)). With co-infusion of [1,3-$^{13}C_2$]BHB and [$^{13}C_6$]-D-glucose brain's selection of fuels can be quantified (Table 1).

4.4. [1-^{13}C]acetate and [$^{13}C_6$]-D-glucose

Previous studies indicate that acetate, the so-called simplest of fats (Ebert et al., 2003) is oxidized in the brain as an energy substrate (Bluml et al, 2002; Lebon et al., 2002). It has been found to be predominantly or exclusively metabolized in glial cells (Nicklas and Clarke, 1969; Badar-Goffer et al., 1990; Cerdan et al., 1990; Waniewski and Martin, 1998; Cruz et al., 2005). Therefore, acetate is usually considered as a marker in the investigation of glial metabolism in the brain (Muir et al., 1986; Waniewski and Martin, 1998). Systemic administration of specific ^{13}C-enriched glucose and/or acetate has been used to study brain energy metabolism and glutamatergic neurotransmission with ^{1}H-decoupled ^{13}C MRS (Taylor et al., 1996; Bluml et al., 2002; Yang et al, 2007). In the present study, [1-^{13}C]acetate produced glutamate, glutamine and aspartate singlets. The resonance signal of [1-^{13}C]acetate appears at 182.15 ppm which partially overlaps with glutamate C5 even at 11.7 Tesla. In separate studies using [2-^{13}C] and [1,2-$^{13}C_2$]acetate we have confirmed that our infusion protocol did not lead to detectable acetate C2 signal at 24.5 ppm. As noted earlier, we observed that the signal intensity of glutamine C5 singlet is much higher than that of glutamate C5 singlet in both Group F and Group G animals. This reversal of the precursor-product relationship between glutamate and glutamine has been detected in the literature (Bluml et al, 2002; Lebon et al, 2002; Yang et al., 2007). Acetate is directly metabolized in glial cells. As a result, glutamine, which resides predominantly in glial cells, is labeled by ^{13}C-labeled acetate first. Via the glutamate-glutamine cycle pathway glutamate, which resides predominantly in glutamatergic neurons, is labeled as a consequence of glutamine hydrolysis by the action of phosphate-activated glutaminase. In Fig. 5 (bottom trace), it was shown that ^{13}C label incorporation from glucose and acetate into glutamate, glutamine and aspartate can be simultaneously detected based on different carboxylic/amide carbon isotopomers.

4.5. Conclusions

The present study has demonstrated the feasibility of detecting metabolism of different energy substrates in brain simultaneously by means of analyzing *in vivo* ^{13}C MRS results from the carboxylic/amide region when different specific ^{13}C-labeled chemicals are administered. An effort to apply this strategy to studying the human brain is currently in progress, which will be helpful for the investigation of brain energy metabolism and neurotransmission under different physiological and pathological conditions.

Acknowledgments

The authors are grateful to Dr. Su Xu, Mr. Christopher Johnson, Drs. Steve Li, Yan Zhang, Jan Willem van der Veen and BuSik Park for their valuable help, and Ioline Henter for editing the manuscript. This work was supported

by the Intramural Research Program of the National Institute of Mental Health, National Institutes of Health, US Department of Health and Human Services (IRP-NIMH-NIH-DHHS).

References

Al-Mamun M, Goto K, Chiba S, Sano H. Responses of plasma acetate metabolism to hop (Humulus lupulus L.) in sheep. Int J Biol Sci. 2009; 5:287–92. [PubMed: 19365576]

Aubert A, Costalat R, Magistretti PJ, Pellerin L. Brain lactate kinetics: Modeling evidence for neuronal lactate uptake upon activation. Proc Natl Sci U S A. 2005; 102:16448–53.

Badar-Goffer RS, Bachelard HS, Morris PG. Cerebral metabolism of acetate and glucose studied by ^{13}C-n.m.r. spectroscopy. A technique for investigating metabolic compartmentation in the brain. Biochem J. 1990; 266:133–9. [PubMed: 1968742]

Beckmann N, Turkalj I, Seelig J, Keller U. ^{13}C NMR for the assessment of human brain glucose metabolism in vivo. Biochemistry. 1991; 30:6362–6. [PubMed: 2054342]

Behar KL, Petroff OA, Prichard JW, Alger JR, Shulman RG. Detection of metabolites in rabbit brain by ^{13}C NMR spectroscopy following administration of [1-^{13}C]glucose. Magn Reson Med. 1986; 3:911–20. [PubMed: 2881185]

Bluml S, Moreno-Torres A, Shic F, Nguy CH, Ross BD. Tricarboxylic acid cycle of glia in the in vivo human brain. NMR Biomed. 2002; 15:1–5. [PubMed: 11840547]

Boumezbeur F, Petersen KF, Cline GW, Mason GF, Behar KL, Shulman GI, et al. The contribution of blood lactate to brain energy metabolism in humans measured by dynamic ^{13}C nuclear magnetic resonance spectroscopy. J Neurosci. 2010; 30:13983–91. [PubMed: 20962220]

Bouzier-Sore AK, Serres S, Canioni P, Merle M. Lactate involvement in neuron-glia metabolic interaction: (13)C-NMR spectroscopy contribution. Biochimie. 2003; 85:841–8. [PubMed: 14652173]

Bouzier-Sore AK, Voisin P, Bouchaud V, Bezancon E, Franconi JM, Pellerin L. Competition between glucose and lactate as oxidative energy substrates in both neurons and astrocytes: a comparative NMR study. Eur J Neurosci. 2006; 24:1687–94. [PubMed: 17004932]

Cerdán S, Kunnecke B, Seelig J. Cerebral metabolism of [1,2-$^{13}C_2$]acetate as detected by in vivo and in vitro ^{13}C NMR. J Biol Chem. 1990; 265:12916–26. [PubMed: 1973931]

Cerdán S, Rodrigues TB, Sierra A, Benito M, Fonseca LL, Fonseca CP, et al. The redox switch/redox coupling hypothesis. Neurochem Int. 2006; 48:523–30. [PubMed: 16530294]

Chen Z, Li SS, Yang J, Letizia D, Shen J. Measurement and automatic correction of high-order B0 inhomogeneity in the rat brain at 11.7 Tesla. Magn Reson Imaging. 2004; 22:835–42. [PubMed: 15234452]

Choi IY, Tkác I, Ugurbil K, Gruetter R. Noninvasive measurements of [1-^{13}C]glycogen concentrations and metabolism in rat brain in vivo. J Neurochem. 1999; 73:1300–8. [PubMed: 10461925]

Cremer JE. Amino Acid Metabolism in Rat Brain Studied with ^{14}C-Labelled Glucose. J Neurochem. 1964; 11:165–85. [PubMed: 14165154]

Cruz NF, Dienel GA. High glycogen levels in brains of rats with minimal environmental stimuli: implications for metabolic contributions of working astrocytes. J Cereb Blood Flow Metab. 2002; 22:1476–89. [PubMed: 12468892]

Cruz NF, Lasater A, Zielke HR, Dienel GA. Activation of astrocytes in brain of conscious rats during acoustic stimulation: acetate utilization in working brain. J Neurochem. 2005; 92:934–47. [PubMed: 15686496]

de Graaf, RA. In vivo NMR spectroscopy: principles and techniques. John Wiley & Sons; Hoboken, NJ: 2007.

Ebert D, Haller RG, Walton ME. Energy contribution of octanoate to intact rat brain metabolism measured by ^{13}C nuclear magnetic resonance spectroscopy. J Neurosci. 2003; 23:5928–35. [PubMed: 12843297]

Ernst RR. Nuclear magnetic double resonance with an incoherent radio-frequency field. J Chem Phys. 1966; 45:3845–61.

Edmond J. Energy metabolism in developing brain cells. Can J Physiol Pharmacol. 1992; 70(Suppl):S118–29. [PubMed: 1295662]

Guzman M, Blazquez C. Is there an astrocyte-neuron ketone body shuttle? Trends Endocrinol Metab. 2001; 12:169–73. [PubMed: 11295573]

Guzman M, Blazquez C. Ketone body synthesis in the brain: possible neuroprotective effects. Prostaglandins Leukot Essent Fatty Acids. 2004; 70:287–92. [PubMed: 14769487]

Hassel B, Sonnewald U, Fonnum F. Glial-neuronal interactions as studied by cerebral metabolism of [2-^{13}C]acetate and [1-^{13}C]glucose: an ex vivo ^{13}C NMR spectroscopic study. J Neurochem. 1995; 64:2773–82. [PubMed: 7760058]

Hawkins RA. Transport of essential nutrients across the blood-brain barrier of individual structures. Fed Proc. 1986; 45:2055–9. [PubMed: 3519289]

Henderson ST. Ketone bodies as a therapeutic for Alzheimer's disease. Neurotherapeutics. 2008; 5:470–80. [PubMed: 18625458]

Lebon V, Petersen KF, Cline GW, Shen J, Mason GF, Dufour S, et al. Astroglial contribution to brain energy metabolism in humans revealed by ^{13}C nuclear magnetic resonance spectroscopy: elucidation of the dominant pathway for neurotransmitter glutamate repletion and measurement of astrocytic oxidative metabolism. J Neurosci. 2002; 22:1523–31. [PubMed: 11880482]

Li S, Shen J. Integrated RF probe for in vivo multinuclear spectroscopy and functional imaging of rat brain using an 11.7 Tesla 89 mm bore vertical microimager. Magma. 2005; 18:119–27. [PubMed: 16007474]

Li S, Yang J, Shen J. Novel strategy for cerebral ^{13}C MRS using very low RF power for proton decoupling. Magn Reson Med. 2007; 57:265–71. [PubMed: 17260369]

Li S, Zhang Y, Wang S, Yang J, Ferraris Araneta M, Farris A, et al. In vivo ^{13}C magnetic resonance spectroscopy of human brain on a clinical 3 T scanner using [2-^{13}C]glucose infusion and low-power stochastic decoupling. Magn Reson Med. 2009; 62:565–73. [PubMed: 19526500]

Lundquist F, Sestoft L, Damgaard SE, Clausen JP, Trap-Jensen J. Utilization of acetate in the human forearm during exercise after ethanol ingestion. J Clin Invest. 1973; 52:3231–5. [PubMed: 4750452]

Magistretti PJ, Pellerin L, Rothman DL, Shulman RG. Energy on demand. Science. 1999; 283:496–7. [PubMed: 9988650]

Malloy CR, Sherry AD, Jeffrey FM. Evaluation of carbon flux and substrate selection through alternate pathways involving the citric acid cycle of the heart by ^{13}C NMR spectroscopy. J Biol Chem. 1988; 263:6964–71. [PubMed: 3284880]

Mangia S, Simpson IA, Vannucci SJ, Carruthers A. The in vivo neuron-to-astrocyte lactate shuttle in human brain: evidence from modeling of measured lactate levels during visual stimulation. J Neurochem. 2009; 109(Suppl 1):55–62. [PubMed: 19393009]

Muir D, Berl S, Clarke DD. Acetate and fluoroacetate as possible markers for glial metabolism in vivo. Brain Res. 1986; 380:336–40. [PubMed: 3756485]

Nehlig A. Brain uptake and metabolism of ketone bodies in animal models. Prostaglandins Leukot Essent Fatty Acids. 2004; 70:265–75. [PubMed: 14769485]

Nicklas WJ, Clarke DD. Decarboxylation studies of glutamate, glutamine, and aspartate from brain labelled with [1-^{14}C]acetate, L-[U-^{14}C]-aspartate, and L-[U-^{14}C]glutamate. J Neurochem. 1969; 16:549–58. [PubMed: 5768211]

Occhipinti R, Somersalo E, Calvetti D. Astrocytes as the glucose shunt for glutamatergic neurons at high activity: an in silico study. J Neurophysiol. 2009; 101:2528–38. [PubMed: 18922953]

O'Neal RM, Koeppe RE, Williams EI. Utilization in vivo of glucose and volatile fatty acids by sheep brain for the synthesis of acidic amino acids. Biochem J. 1966; 101:591–7. [PubMed: 16742430]

Owen OE, Morgan AP, Kemp HG, Sullivan JM, Herrera MG, Cahill GF Jr. Brain metabolism during fasting. J Clin Invest. 1967; 46:1589–95. [PubMed: 6061736]

Pan JW, de Graaf RA, Petersen KF, Shulman GI, Hetherington HP, Rothman DL. [2,4-$^{13}C_2$]-beta-Hydroxybutyrate metabolism in human brain. J Cereb Blood Flow Metab. 2002; 22:890–8. [PubMed: 12142574]

Pearson H, Gust D, Armitage IM, Huber H, Roberts JD, Stark RE, et al. Nuclear magnetic resonance spectroscopy: reinvestigation of carbon-13 spin-lattice relaxation time measurements of amino acids. Proc Natl Acad Sci U S A. 1975; 72:1599–601. [PubMed: 165516]

Pellerin L, Magistretti PJ. How to balance the brain energy budget while spending glucose differently. J Physiol. 2003; 546:325. [PubMed: 12527720]

Prichard JW. What the clinician can learn from MRS lactate measurements. NMR Biomed. 1991; 4:99–102. [PubMed: 1859788]

Rumpel C. Does burning of harvestinig residues increase soil carbon storage? J Soil Sc Plant Nutr. 2008; 8:44–51.

Schurr A. Lactate: the ultimate cerebral oxidative energy substrate? J Cereb Blood Flow Metab. 2006; 26:142–52. [PubMed: 15973352]

Sibson NR, Dhankhar A, Mason GF, Behar KL, Rothman DL, Shulman RG. In vivo ^{13}C NMR measurements of cerebral glutamine synthesis as evidence for glutamateglutamine cycling. Proc Natl Acad Sci USA. 1997; 94:2699–704. [PubMed: 9122259]

Shen J, Novotny EJ, Rothman DL. In vivo lactate and beta-hydroxybutyrate editing using a pure-phase refocusing pulse train. Magn Reson Med. 1998; 40:783–8. [PubMed: 9797163]

Shen J, Petersen KF, Behar KL, Brown P, Nixon TW, Mason GF, et al. Determination of the rate of the glutamate/glutamine cycle in the human brain by in vivo ^{13}C NMR. Proc Natl Acad Sci U S A. 1999; 96:8235–40. [PubMed: 10393978]

Sykes JE, Lopes-Cardozo M, Van Den Bergh SG. Substrate utilization for energy production and lipid synthesis in oligodendrocyte-enriched cultures prepared from rat brain. Neurochem Int. 1986; 8:67–75. [PubMed: 20493031]

Taylor A, McLean M, Morris P, Bachelard H. Approaches to studies on neuronal/glial relationships by ^{13}C-MRS analysis. Dev Neurosci. 1996; 18:434–42. [PubMed: 8940616]

Uehara T, Sumiyoshi T, Itoh H, Kurata K. Lactate production and neurotransmitters; evidence from microdialysis studies. Pharmacol Biochem Behav. 2008; 90:273–81. [PubMed: 18502489]

Urrila AS, Hakkarainen A, Heikkinen S, Vuori K, Stenberg D, Hakkinen AM, et al. Stimulus-induced brain lactate: effects of aging and prolonged wakefulness. J Sleep Res. 2004; 13:111–9. [PubMed: 15175090]

Veech RL, Chance B, Kashiwaya Y, Lardy HA, Cahill GF Jr. Ketone bodies, potential therapeutic uses. IUBMB Life. 2001; 51:241–7. [PubMed: 11569918]

Waagepetersen HS, Bakken IJ, Larsson OM, Sonnewald U, Schousboe A. Comparison of lactate and glucose metabolism in cultured neocortical neurons and astrocytes using ^{13}C-NMR spectroscopy. Dev Neurosci. 1998; 20:310–20. [PubMed: 9778567]

Waniewski RA, Martin DL. Preferential utilization of acetate by astrocytes is attributable to transport. J Neurosci. 1998; 18:5225–33. [PubMed: 9651205]

Wilson, MA. NMR-Techniques and Application in Geochemistry and Soil Chemistry. Pergamin Press; Oxford: 1987.

Xu S, Shen J. In vivo dynamic turnover of cerebral ^{13}C isotopomers from [U-^{13}C]glucose. J Magn Reson. 2006; 182:221–8. [PubMed: 16859940]

Yang J, Johnson C, Shen J. Detection of reduced GABA synthesis following inhibition of GABA transaminase using in vivo magnetic resonance signal of [^{13}C]GABA C1. J Neurosci Methods. 2009; 182:236–43. [PubMed: 19540876]

Yang J, Li SS, Bacher J, Shen J. Quantification of cortical GABA-glutamine cycling rate using in vivo magnetic resonance signal of [2-^{13}C]GABA derived from glia-specific substrate [2-^{13}C]acetate. Neurochem Int. 2007; 50:371–8. [PubMed: 17056156]

Zakhari S. Overview: how is alcohol metabolized by the body? Alcohol Res Health. 2006; 29:245–54. [PubMed: 17718403]

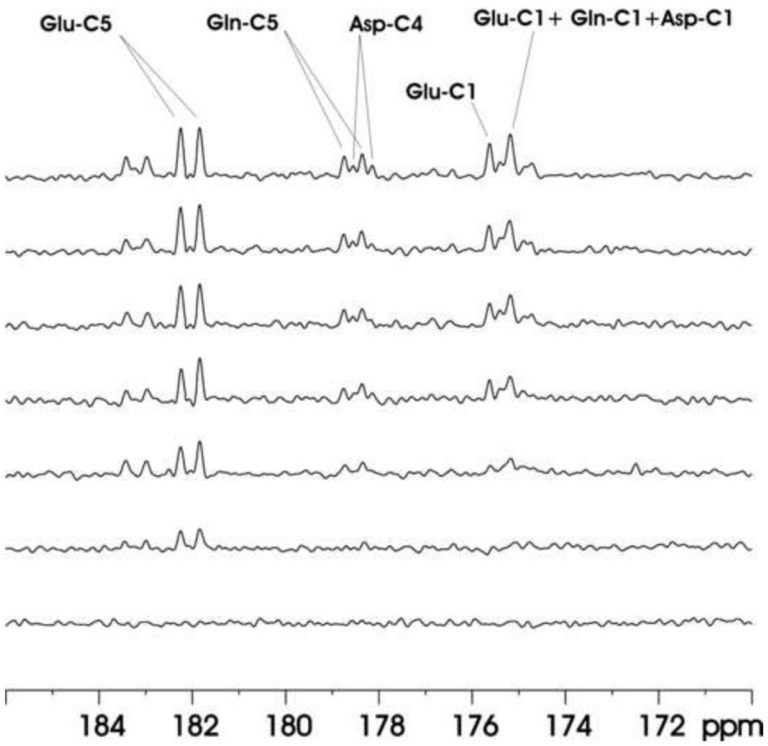

Figure 1.

Baseline (bottom trace) and time-course (120 minutes) ^{13}C MRS spectra acquired from an individual rat brain during intravenous infusion of [$^{13}C_6$]-D-glucose. Each spectrum was averaged for 20 minutes. Parameters for data processing: lb = −15, gb = 0.12. Glu-C5: glutamate C5, Gln-C5: glutamine C5, Asp-C4: aspartate C4, Glu-C1: glutamate C1, Gln-C1: glutamine C1.

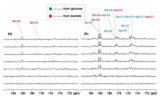

Figure 2.

(a) Baseline (bottom trace) and time-course (120 minutes) ^{13}C MRS spectra acquired from an individual rat brain during intravenous infusion of [2-^{13}C] lactate. (b) Baseline (bottom trace) and time-course (120 minutes) ^{13}C MRS spectra acquired from an individual rat brain during intravenous co-infusion of [2-^{13}C]lactate and [$^{13}C_6$]-D-glucose. Each individual spectrum was averaged for 20 minutes. Parameters for data processing: lb = −15, gb = 0.12. Glu-C5: glutamate C5, Gln-C5: glutamine C5, Asp-C4: aspartate C4, Glu-C1: glutamate C1, Asp-C1: aspartate C1, Gln-C1: glutamine C1. Green: resonance lines originated from [$^{13}C_6$]-D-glucose; Red: resonance lines originated from [2-^{13}C] lactate.

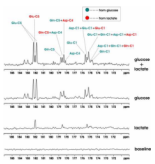

Figure 3.

Summed in vivo ^{13}C MRS spectra. Baseline: no significant interfering signals were detected in the spectral region of interest. Lactate: only singlets of glutamate, glutamine and aspartate were detected during intravenous infusion of [2-^{13}C]lactate. Glucose: only doublets were detected for glutamate C5, glutamine C5 and aspartate C4 during intravenous infusion of [$^{13}C_6$]-D-glucose. Glucose+lactate: both doublets and singlets were detected for glutamate C5, glutamine C5 and aspartate C4 during intravenous co-infusion of [$^{13}C_6$]-D-glucose and [2-^{13}C]lactate. Each spectrum was averaged over the 0~180 minutes infusion period. Lactate: [2-^{13}C] lactate, glucose: [$^{13}C_6$]-D-glucose. Parameters for data processing: lb = −15, gb = 0.12. Glu-C5: glutamate C5, Gln-C5: glutamine C5, Asp-C4: aspartate C4, Glu-C1: glutamate C1, Asp-C1: aspartate C1, Gln-C1: glutamine C1. Green: resonance lines originated from [$^{13}C_6$]-D-glucose; Red: resonance lines originated from [2-^{13}C] lactate.

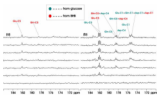

Figure 4.

(a) Baseline (bottom trace) and time-course (120 minutes) ^{13}C MRS spectra acquired from an individual rat brain during intravenous infusion of [1,3-$^{13}C_2$] BHB. (b) Baseline (bottom trace) and time-course (120 minutes) ^{13}C MRS spectra acquired from an individual rat brain during intravenous co-infusion of [1,3-$^{13}C_2$] BHB and [$^{13}C_6$]-D-glucose. Each individual spectrum was averaged for 20 minutes. Parameters for data processing: lb = −15, gb = 0.12. Glu-C5: glutamate C5, Gln-C5: glutamine C5, Asp-C4: aspartate C4, Glu-C1: glutamate C1, Asp-C1: aspartate C1, Gln-C1: glutamine C1. Green: resonance lines originated from [$^{13}C_6$]-D-glucose; Red: resonance lines originated from [2-^{13}C] lactate.

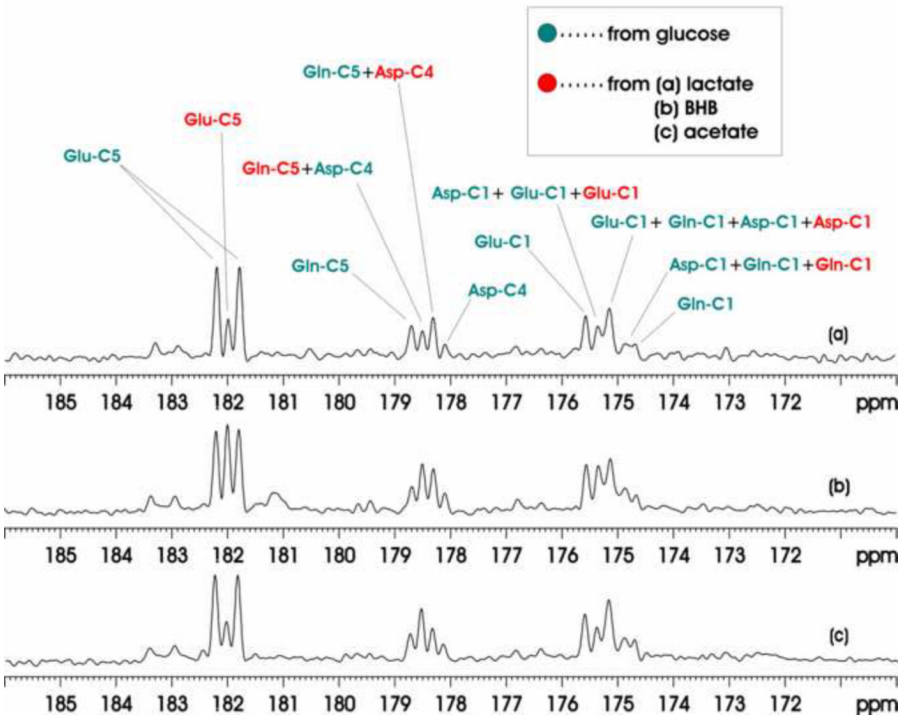

Figure 5.

Accumulated in vivo ^{13}C MRS spectra of intravenous co-infusions of [$^{13}C_6$]-D-glucose + [2-^{13}C]lactate (**a**), [$^{13}C_6$]-D-glucose + [1,3-$^{13}C_2$]BHB [(**b**), and [$^{13}C_6$]-D-glucose + [1-^{13}C]acetate (**c**). Each spectrum was averaged over the 0–180 minutes infusion period from an individual rat brain. Parameters for data processing: lb = −15, gb = 0.12. Glu-C5: glutamate C5, Gln-C5: glutamine C5, Asp-C4: aspartate C4, Glu-C1: glutamate C1, Asp-C1: aspartate C1, Gln-C1: glutamine C1. Green: resonance lines originated from [$^{13}C_6$]-D-glucose; Red: resonance lines originated from [2-^{13}C] lactate.

Table 1

Contribution to cerebral metabolism from different ^{13}C-labeled substrates

Co-infusion	$[GluC5]_{Glc}/[GluC5]_{2nd}$*	$[GlnC5]_{Glc}/[GlnC5]_{2nd}$	$[GluC5+GlnC5+AspC4]_{Glc}/[GluC5+GlnC5+AspC4]_{2nd}$
Glc+Lac (n=10)	4.23 ± 0.30	7.50 ± 0.31	5.11 ± 0.58
Glc+BHB (n=9)	2.34 ± 0.21	3.77 ± 0.49	3.16 ± 0.20
Glc+Ac (n=10)	5.24 ± 0.48	1.80 ± 0.23	3.54 ± 0.34

*Concentration ratio of ^{13}C-labeled metabolites at 180 min after the initiation of co-infusion. "2nd" represents lactate (Lac) or BHB or acetate (Ac). All ratios were reported as mean ± SD.